NCREE NEWSLETTER

March 2014 VOL. 9 NO. 1



CONTENTS

- Development of Sloped Rolling-Based Isolation Devices for Seismic Protection of Important Equipment and Facilities
- Comparison of Distribution Methods for Viscous Damping Coefficients to Buildings
- Development and Application of a Seismic Multiple Shaking Table Test System
- Off-line Simulation of On-site Peak Ground Acceleration Estimation based on Support Vector Regression
- Using Wireless Sensors to Avoid False Alarms in an Earthquake Early Warning System
- Experimental Studies on the Seismic Behavior of Piping Systems in Critical Facilities
- International Communication of Research and Development of Earthquake Engineering between Taiwan and Haiti
- Introduction of Hydraulics Experiments for Pier Scouring

DIRECTOR

Kuo-Chun Chang

EDITORS

Shiang-Jung Wang

Ting-Yu Hsu

National Center for Research on Earthquake Engineering

Development of Sloped Rolling-Based Isolation Devices for Seismic Protection of Important Equipment and Facilities

Shiang-Jung Wang, Yin-Han Yang, Chia-Yi Shiau, Wang-Chuen Lin, Jenn-Shin Hwang, Kuo-Chun Chang, NCREE

Performance-based design emphasizes that the seismic performance of buildings depends on not only the seismic-resistant capability of structural components, but also the functionality of the nonstructural contents during or after earthquakes. In this study, a sloped multi-roller isolation device for seismic protection of critical equipment or facilities, as shown in the schematic drawing of Fig. 1, is developed.

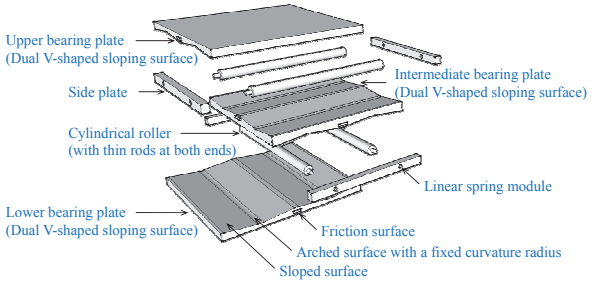


Fig. 1. Schematic view of the sloped multi-roller isolation device

The rolling mechanisms of two pairs of mutually orthogonal rollers provide a stable in-plane seismic isolation function. By cooperating with the side plates, the synchronous movement for the rollers in each principle horizontal direction can effectively prevent undesired sliding motions between the rollers and bearing plates as well as undesired overturning motions of the isolation device. With this multi-roller design, a better stability performance can be achieved compared to the conventional single-roller design. In addition to the rolling friction engaged in energy absorption, the adjustable linear spring modules embedded in the side plates can generate the normal forces required to supply additional sliding friction forces between the side plates and bearing plates. This built-in damping mechanism can facilitate the isolation device to suppress excessive displacement responses and stop rolling motion during and after excitations, respectively. To prevent some undesired spikes in both the horizontal and vertical acceleration responses introduced by pounding between the rollers and the inclined surfaces, an arc rolling range with a fixed curvature radius, which is much larger than the roller radius, is provided at the intersection of two inclines of the V-shaped surfaces of the bearing plates.

The seismic performance of the sloped multi-roller isolation device with the abovementioned refinements was experimentally investigated for a seismically isolated raised floor system. For the four isolation devices underneath the raised floor system, the sloping angle of the V-shaped surfaces of the bearing plates is designed to be 6°, and the normal force for sliding friction applied to each side plate is approximately 332.52N. The total mass of the raised floor system is 1420N-sec^2/m. The to-be-protected equipment above the seismically isolated raised floor system is simulated by lead blocks with a total mass of 1000N-sec^2/m; the experimental setup is shown in Fig. 2. Two generated bilateral acceleration histories, denoted as AC156-TAP090 and AC156-TCU054, compatible with the required response spectra (RRS) are adopted in the seismic simulation tests.



Fig. 2. Installation photos of the seismically isolated raised floor system

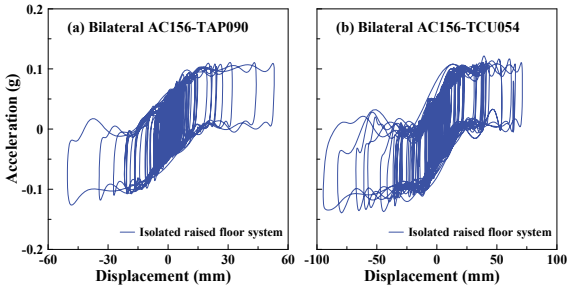


Fig. 3. Experimental results of the seismically isolated raised floor system: The hysteresis loops are in the *x* direction

As observed in Fig. 3, the maximum acceleration response transmitted to the seismically isolated raised floor system can still reveal an acceptably steady level. As the built-in sliding friction is engaged, the hysteresis loops reveal a better energy dissipation capability.

In this study, the high efficiency of employing sloped multi-roller isolation devices in reducing seismic demands (or damage potential) of protected objects is experimentally verified. The isolation device features a standardized design irrespective of input motions, which is one of the most important concerns for critical equipment or facilities if the maximum acceleration response is selected as the seismic performance criterion. In Taiwan, the sloped multi-roller isolation devices have been practically applied to the seismic protection of critical equipment and facilities in a number of industries and organizations, as shown in Fig. 4.

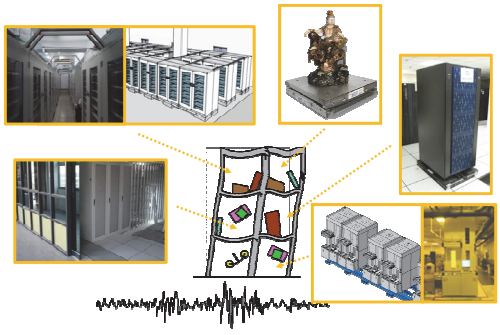


Fig. 4. Practical applications of sloped multi-roller isolation devices

Comparison of Distribution Methods for Viscous Damping Coefficients to Buildings

Wang-Chuen Lin, Assistant Researcher, NCREE
Jenn-Shin Hwang, Professor, and NCREE

Current design guidelines for the incorporation of viscous dampers into building structures are based on the total effective damping ratio contributed by the added viscous dampers. However, no rational distribution methods are readily available for distributing the damping coefficients along the height of the structure corresponding to the desired added effective damping ratio. Recently, many studies have placed emphasis on the optimal design of dampers in a building using methods such as genetic algorithms. In addition, a simplified sequential search algorithm (SSSA) has been proposed by Garcia. For simplicity and convenience in current design, practicing engineers claim that the damping coefficients of the linear viscous dampers of each story are identical, *i.e.*, a uniform distribution (UD). Another existing method that has been suggested is to distribute the damping coefficients in proportion to the story shear force of a building, *i.e.*, a story shear proportional distribution (SSPD). This article examines two simple and non-repetitive design formulas that assign a damping coefficient to each story that is proportional to the story shear strain energy.

The design formula provided by FEMA 273/356 for calculating the supplemental damping ratio provided by linear viscous dampers is specified by:

$$\xi_d = T\sum_j C_j f_j^{\,2}\phi_{rj}^{\,2} \Big/ 4\pi\sum_i m_i\phi_i^{\,2} \qquad (1)$$

Raggett proposed that the contribution of the element-damping ratio to the system-damping ratio is equal to the element-damping ratio weighted by the element strain energy divided by the total system strain energy. According to Raggett's concept, the design formula in this study for distributing the total damping coefficient to each story based on the story shear strain energy (SSSE) can be expressed as:

$$C_j = 4\pi\xi_d\phi_{rj}S_j\sum_j m_j\phi_j^2 \Big/ T\sum_j \phi_{rj}S_j\left(f_j\phi_{rj}\right)^2 \quad , \quad S_j = \sum_{i=j}^{Roof} m_i\phi_i \qquad (2)$$

In order to make more efficient use of viscous dampers, the total damping coefficient is distributed only to those stories with a shear strain energy larger than the average story shear strain energy. The distribution based on the SSSE to efficient story (SSSEES) can be derived as:

$$C_j = 4\pi\xi_d\phi_{rj}S_j\sum_j m_j\phi_j^2 \Big/ T\sum_j^k \phi_{rj}S_j\left(f_j\phi_{rj}\right)^2 \qquad (3)$$

where k is the number of stories with a story shear strain energy larger than the average story shear strain energy.

The distribution formulas corresponding to the UD, SSPD, SSSE, SSSEES, and SSSA are examined. In this study, it should be noted that an incremental damping coefficient of 50 kN s/m is adopted if the repetitive search procedure of SSSA is applied. In order to compare different distribution methods, the sectional dimensions of the columns and beams of a 10-story building with two soft stories is summarized in Fig. 1. It is assumed that the inherent damping ratio of the structure is 5%, and that the structure is designed to provide a desired damping ratio of 10% for supplemental linear viscous dampers. The damping coefficients corresponding to the five distribution methods for the building structure are summarized in Table 1.

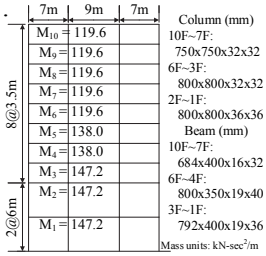


Fig.1. Properties of the example frame

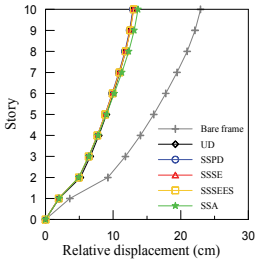


Fig. 2. Maximum seismic responses of the example frame

Assuming the building remains elastic, the dynamic response histories of the structure subjected to the 40% TCU065 of the 1999 Taiwan Chi-Chi earthquake (PGA = 0.304 g) are obtained using SAP2000. The seismic responses are compared in Figure 2, and the distribution of the maximum damper forces along the height of the structure is shown in Table 2. From Fig. 2, it is observed that the maximum lateral displacements of the structure with added dampers are almost the same. According to the comparisons of damping coefficients and maximum damper force, the results show that the greatest damper force demand over the least number of stories is found using SSSA. The distribution methods using the UD and the SSPD with more total damping coefficients lead to greater total damper force capacity, but the seismic responses do not have a better energy dissipation behavior. On the other hand, the distribution methods using SSSE and SSSEES require fewer total damping coefficients and less damper force to provide a similar effect as the others.

Table 1. Damping coefficients of the example frame (kN s/m)

Story	UD	SSPD	SSSE	SSSEES	SSSA
10	5525	857	163	0	0
9	5525	1684	451	0	0
8	5525	2468	854	0	0
7	5525	3197	1244	0	0
6	5525	3864	1588	0	0
5	5525	4558	2101	0	0
4	5525	5168	2697	2833	0
3	5525	5716	3510	3688	0
2	5525	6145	8213	8628	12000
1	5525	6311	5371	5643	0
Total	55250	39968	26192	20792	12000

Table 2. Maximum damper forces of the example frame

Story	UD	SSPD	SSSE	SSSEES	SSSA
10	118	21	5	0	0
9	189	63	18	0	0
8	257	120	44	0	0
7	289	170	69	0	0
6	304	214	90	0	0
5	350	290	138	0	0
4	407	382	206	217	0
3	491	503	313	329	0
2	1087	1188	1546	1616	2300
1	731	821	712	748	0
Total	4222	3770	3140	2910	2300

According to the proportionality of the SSSE in this study, two simple and non-repetitive formulas for distributing the total damping coefficients to each story have been derived. Overall, after comparing various distribution methods in the study, SSSEES may provide a more satisfactory solution for the practical design of viscous dampers.

Development and Application of a Seismic Multiple Shaking Table Test System

Pei-Ching Chen, Assistant Researcher, Pei-Yang Lin, Research Fellow, Hung-Wei Chiang, Assistant Researcher, NCREE

Shaking table testing is regarded as one of the most robust experimental methods for investigating structural dynamic responses in earthquake engineering. The entire tested structure is mounted on the table and subjected to prescribed ground motions in real time; as a result, seismic responses and rate-dependent behavior can be fairly represented. However, long-span bridges and piping systems, by nature, are subjected to spatially varying earthquake ground motions, which cannot be reproduced using traditional shaking tables. Therefore, a multiple shaking table test system, composed two or more individual shaking tables, is essential to carry out these tests for specific research purposes. By allocating different configurations to each individual shaking table, this test system can meet a wide range of experimental requirements in the laboratory.

Two individual uni-axial shaking tables have been constructed at NCREE since 2012. The first table (shaking table A) is made of steel with dimensions of 2500 mm × 1700 mm. The linear guide way system is adopted as the sliding mechanism between the platen and a steel reaction frame. Two guide ways are installed at the edge of the steel reaction frame in the longitudinal direction. There are four carts for each guide way to resist the overturning moment from the platen above. An existing MTS servo-hydraulic actuator with ±250-kN force and ±250-mm stroke capacities is used. The maximum flow rate for the servo valve is 90 gpm. The allowable payload of shaking table A is 20 kN. The second table (shaking table B) is made of aluminum with dimensions of 1000 mm × 1000 mm. Two hydrostatic bearings are used for the sliding mechanism in order to reduce the friction force. Furthermore, an existing MTS servo-hydraulic actuator is used to drive the table. The force and stroke capacity of the actuator are ±25 kN and ±75 mm, respectively. The maximum flow rate for the servo valve is 15 gpm. The payload is up to 5 kN, which is restricted by the loading capacity of the hydrostatic bearings. The two shaking tables are operated by using a digital PID controller provided by a manufacturer in Taiwan.

Shaking table control is a challenging issue because the desired signal is an acceleration record while actuators are mostly driven via displacement control. Meanwhile, the dynamics of the tested specimen lead to pronounced control–structure interaction, which is generally nonlinear, especially when damage occurs to the specimen during a test. As a result, it is difficult to accurately reproduce a prescribed acceleration time history over a broad frequency using an inner-loop PID controller. An outer-loop controller can be employed in the servo-hydraulic system control loop to change the dynamics of the overall test system. In this research, the outer-loop control framework is designed to improve the acceleration tracking and system robustness with regard to nonlinearities.

In order to design and implement the outer-loop controller into the original shaking table control loop, dSPACE is adopted as it is directly interfaced with MATLAB/Simulink running on a computer. A DS1103 controller board provides fast I/O for applications. By using Real-Time Interface (RTI), the outer-loop controller can be fully designed and analyzed from the Simulink block diagram environment. All the I/O can also be easily configured using the RTI. This programmed diagram is then converted to real-time C code, cross–compiled, and downloaded to the controller board. Meanwhile, the control panel for the multiple shaking table test system can be designed using ControlDesk, a graphical user interface, for tuning controller parameters, collecting data, and displaying experimental results in real time. The schematic layout for the multiple shaking table control system is illustrated in Fig. 1.

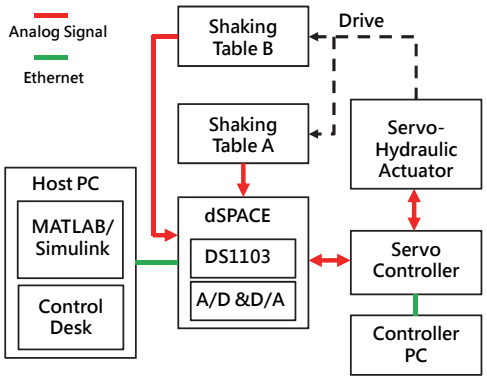


Fig.1. Control framework for the multiple shaking table test system

Up to now, several validation tests have been conducted for each individual shaking table using the feedforward displacement compensation method. The experimental results demonstrate that the outer-loop controller improves the acceleration tracking accuracy, especially in the high-frequency range (15–20 Hz), compared with the original PID control scheme. Different control strategies will be tested in the future, for example, dual feedforward controllers using both displacement and acceleration feedback, or the loop-shaping method for increasing the robustness of the system. Finally, a long-span bridge specimen will be designed and tested to verify the control framework of the multiple shaking table test system.

Off-line Simulation of On-site Peak Ground Acceleration Estimation based on Support Vector Regression

Ting-Yu Hsu, Shieh-Kung Huang, Hung-Wei Chiang, Pei-Yang Lin, Kung-Chun Lu, Tao-Ming Chang, Shyu-Yu Wu NCREE
Kuo-Liang Wen, National Central University

In order to reduce economic and human loss due to a strong earthquake, researchers have developed techniques to predict the seismic intensity (SI) of upcoming earthquake by using P-wave features. However, huge economic costs of company or decrease of response time owing to false alarm of the earthquake early warning system (EEWS) must be prevented. Since the prediction method equipped in most of the on-site stations of NCREE is the method based on estimation of magnitude and hypocenter distance using P-wave features (TauC-Pd method), the performance of on-site EEWS stations based on the support vector regression method (SVR) remains unknown, although the prediction accuracy rate of SVR method is up to 99.2% when applying to the data of Taiwan Strong Motion Instrumentation Program (TSMIP). Thus, in this study, we try to estimate the on-line performance of SVR by using data of the on-site stations via off-line simulation and then compare the performance with TauC-Pd method.

In SVR, the predicted peak ground acceleration (PGA) is estimated by using six P-wave features extracted from the first three seconds of vertical ground acceleration based on a regression model established in advance. These features are predominant period (TauC), peak acceleration (P_a), peak velocity (P_v), peak displacement (P_d), cumulative absolute velocity (CAV) and integral of the squared velocity (IV2).

The on-site EEWS stations are selected for off-line simulation, and a total of 15,347 recorded earthquake data were collected from 2011 to 2013. These stations are located at the I-Lan elementary school, Gang-Ping elementary school, Guang-Fu elementary school, Yu-Dong junior high school and Nan-An junior high school. The reliability of off-line simulation was verified by using earthquake data of Nan-An junior high school where the online SVR method was equipped from August 14, 2012 to November 3, 2013. Finally, off-line simulation is proved extremely reliable since the correlation coefficient between on-line predicted PGA and off-line predicted PGA based on SVR method was up to 0.999999889.

Fig. 1 represents the relationship between measured PGA and predicted PGA in off-line simulation using SVR method in Yu-Dong station. X-axis is the measured PGA, Y-axis is the predicted PGA. In Fig.1, the triangles represent the earthquake data correlated to some of Central Weather Bureau (CWB), and the circles represent the rest. In on-site stations, the EEWS is alarming if $SI_{predicted} \geqq 4$. Thus, the false positive region is defined as the area where $SI_{predicted} \geqq 4$ and $SI_{predicted} - SI_{measured} \geqq 2$, as the upper left area enclosed by black dash lines in Fig 1. Similarly, the false negative region is defined as the area where $SI_{measured} \geqq 4$ and $SI_{measured} - SI_{predicted} \geqq 2$, as the lower right area enclosed by black dash lines in Fig. 1.

This study defined the Prediction Accuracy Rate (PAR), False Positive Rate (FPR) and False Negative Rate (FNR) as indices to check the reliability of predicted PGA.

$$PAR(\%) = \frac{\text{The number of } |SI_{predicted} - SI_{measured}| \leq 1}{\text{The number of total earthquake data}}$$

$$FPR(\%) = \frac{\text{The number of earthquake data within false positive region}}{\text{The number of earthquake data with } SI_{predicted} \geq 4}$$

$$FNR(\%) = \frac{\text{The number of earthquake data within false negative region}}{\text{The number of earthquake data with } SI_{measured} \geq 4}$$

The comparison of the results of both SVR method (off-line) and TauC-Pd method (on-line) are shown in Table 1.

In general, SVR is far superior to TauC-Pd in PAR (99.4% versus 67.3%) and in FPR (7.7% versus 67.3%). The FNR of both methods are zero, partly due to limited number of earthquake data with $SI_{measured} \geqq 2$. Furthermore, the standard deviation (STD) of PAR is suggested to be the stable index of prediction method. The stability of SVR (1.2%) is better than TauC-Pd (23.2%). In the future, the main task is to avoid false positive alarm which is mostly originated from disturbance of non-seismic events.

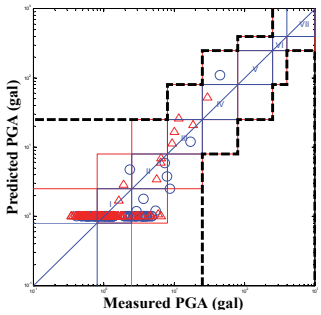


Fig. 1. Measured PGA versus predicted PGA

Table 1. Comparison of results of both methods

Indices \ On-site Station		I-Lan_1	I-Lan_2	Nan-An	Gang-Ping	Guang-Fu	Yu-Dong	Average (STD)
PAR (%)	SVM	100	99.9	99.8	100	96.9	100	99.4 (1.2)
	TauC-Pd	82.0	94.4	74.7	74.7	78.0	26.8	71.8 (23.2)
FPR (%)	SVM	0	20.0	3.8	0	22.2	0	7.7 (10.5)
	TauC-Pd	77.8	90.0	68.2	0	77.1	90.4	67.3 (34.0)

Using Wireless Sensors to Avoid False Alarms in an Earthquake Early Warning System

Kung-Chun Lu, Hong-Wei Chiang, Assistant Researcher, NCREE
Pei-Yang Lin, Research Fellow, Shieh-Kung Huang, Assistant Researcher, NCREE

This research is focused on solving the false alarm problem of the on-site earthquake early warning system (EEWS) and proposed a new concept called "sub-regional EEWS" is proposed. The sub-regional EEWS merges the concepts of both regional and on-site EEWS; the regional EEWS is accurate owing to multiple data verification, and the on-site EEWS is fast by avoiding data communication. The sub-regional EEWS inherits the architecture of the on-site EEWS and extends to consider sub-site information from other positions. The concepts of wireless sensors, a wireless sensor network, and embedded parallel data pre-processing are adopted in this system to avoid the time delay in data collection and computation. The wireless sensing unit applied in the sub-regional EEWS is an NTU-WSU, whose basic architecture is from the Stanford University prototype, WiMMS. This research will demonstrate a successful application of a wireless sensor in an EEWS, provide working detail on system integration, and show the overall system performance of the sub-regional EEWS.

The sub-regional EEWS is produced to prevent false alarms in the on-site EEWS and to gain longer warning times for seismic reactions. It uses the features of the regional and on-site EEWSs that are fast and accurate. In order to preserve the quick response feature of the on-site EEWS, the sub-regional EEWS inherits the basic architecture of the on-site EEWS, which is based on local ground acceleration to judge the seismic contents. To avoid false alarms in the on-site EEWS, the sub-regional EEWS adopts wireless sensing technology to receive and consider multiple ground acceleration signals in a customized region. The false alarm is eliminated through cross-verification of the results of different sites and the quick response feature is guaranteed through wireless communication and the parallel embedded computing of the wireless sensor.

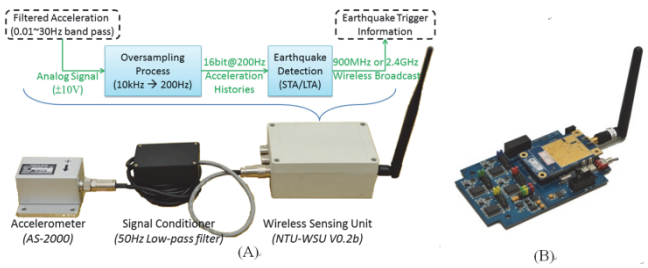


Fig. 1. (A) The framework of the earthquake event detector. (B) The NTU-WSU V0.2b

In this research, the wireless sensing unit, NTU-WSU V0.2b, is adopted, the STA/LTA algorithm is embedded into it, and this is called the earthquake event detector in the sub-regional EEWS. The architecture of the earthquake event detector is shown in Fig. 1(A). The ground acceleration is transduced by a force-balanced accelerometer, AS-2000, a band-pass analog filter (0.01 Hz – 30 Hz) is used to optimize the acceleration signal, and finally the filtered voltage signal is digitalized and sampled by the NTU-WSU. To enhance the sampling performance, the first process in the NTU-WSU is an oversampling process, which captures the signal at ultra-high speed (10 kHz), then down sample to the required sampling rate (200 Hz). The second step in the NTU-WSU is earthquake detection (STA/LTA). Finally, the earthquake trigger information is generated and broadcasted wirelessly. Fig. 1(B) shows the hardware of the NTU-WSU V0.2b.

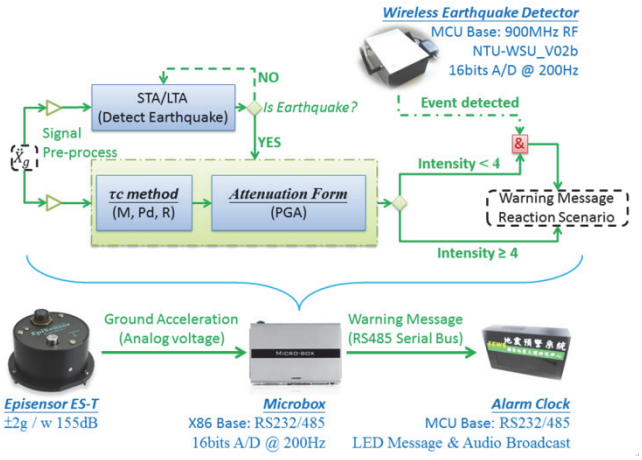


Fig. 2. The framework of the sub-regional EEWS

The framework of the sub-regional EEWS is shown in Fig. 2. An extra judgment is added after the PGA prediction; if the predicted intensity is larger than level 4, the warning action is achieved directly; otherwise, if the predicted intensity is smaller than level 4, then the warning action is achieved after verifying it with the results of the wireless earthquake event detector. This logical arrangement guarantees that a warning message will be issued under serious seismic threats, even if the wireless communication fails and eliminates the false alarm under minor seismic events.

The wireless sensing unit (NTU-WSU V0.2b) provides two important features, the wireless sensor network and parallelized embedded computing, and allows the concept of the sub-regional EEWS to be realized. Via communication of the wireless sensor network, the sub-regional EEWS implements a regional evaluation with almost no time delay in data communication. In other words, the parallel embedded computing on the microcontroller of the NTU-WSU shortens the computing time of the entire EEWS analysis. Finally, the sub-regional EEWS retains the quick response of the on-site EEWS and enhances accuracy close to the regional EEWS.

Experimental Studies on the Seismic Behavior of Piping Systems in Critical Facilities

Juin-Fu Chai, Research Fellow, Fan-Ru Lin, Zhen-Yu Lin, Zhen-Yu Lai, Assistant Researcher, NCREE

Among the problems caused by seismic damage to nonstructural components, water leakage or flooding resulting from broken sprinkler piping systems is of importance in critical facilities, owing to its effects on the room fixtures below that could be related to the functionality of the facilities. This occurred at the Olive View, Holly Cross Medical Center, and Northridge hospitals in the San Fernando Valley during the 1994 Northridge earthquake. On the other hand, according to the seismic risk assessment results presented in the Final Safety Analysis Report (FSAR) for a nuclear power plant (NPP) in Taiwan, the failure of the Residual Heat Removal (RHR) piping system occurs in the two accident sequences with the highest contributions to core damage. Therefore, analysis of the RHR piping system was emphasized in the seismic probabilistic risk assessment (SPRA) of an NPP.

In order to conduct a more accurate fragility analysis in the SPRA for the critical piping systems mentioned above, it is necessary to establish reliable numerical models of the piping system. However, the common numerical models for piping joints, such as flanges and couplings, cannot simulate the non-linear behavior very accurately. In recent research conducted by the NCREE, experimental studies were completed to investigate the mechanical behavior of piping joints under cyclic pure bending and to verify the accuracy of finite element method (FEM) analysis. The final purpose of this research is to propose acceptable simplified models of piping joints to improve the efficiency of numerical analysis for critical piping systems. The other purpose is to provide an effective method to improve the seismic performance of critical piping. Therefore, the effects of seismic restraint devices were also discussed through shaking table tests.

Sprinkler Piping Systems in Hospitals

This study involved component tests and subsystem tests for typical configurations of sprinkler piping in hospitals. Cyclic loading tests were conducted to investigate the inelastic behavior of components, including concrete anchorages, screwed fittings of small-bore piping, and mechanical couplings (Fig. 1). Part of the horizontal piping system of a sprinkler piping from a hospital seismically damaged during the 2010 Jiashian earthquake was reproduced to conduct shaking table tests. Furthermore, the horizontal piping subsystems with seismic-resistant devices such as braces, flexible pipes, and mechanical couplings were tested. The test results showed that the main cause of the damaged case was the poor shear capacity of the screwed fitting of the small-bore tee branch. The optimum improvement strategy to achieve a higher nonstructural performance level for the horizontal piping subsystem is to strengthen the main pipe with braces and to decrease shear demands on the tee branch by flexible pipes. The hysteresis loops and failure modes of the piping joints were further investigated and were used to conduct numerical analysis of the sprinkler piping.

Piping Joints of RHR Systems in NPPs

The seismic performance of the RHR piping system depends on the capacity of its components, such as its support, flange joints, and reducers. Pure bending tests with four-point cyclic loading were conducted for sample flange joints and reducers, to investigate their mechanical behaviors. Detailed numerical models of a flange joint and reducer were also established using ABAQUS and SAP2000 software (Fig. 2). The hysteresis loops and failure modes identified from the tests are in good agreement with the results from numerical analysis. A preliminary simplified model of the flange joint was also proposed in this study to improve the efficiency of numerical analysis for the RHR piping system.

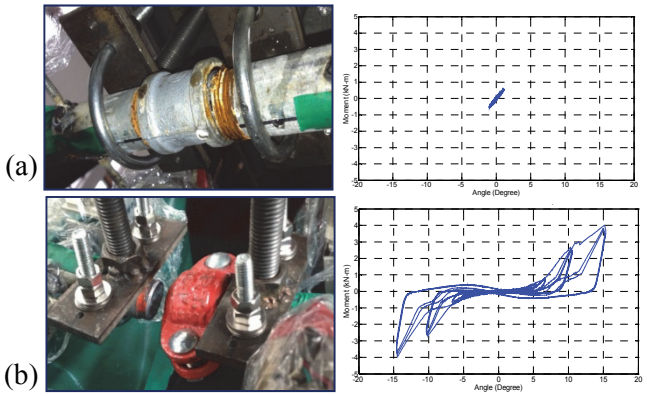


Fig.1. Damage states and moment–θ curves of the sprinkler piping joints: (a) screwed fitting and (b) flexible coupling

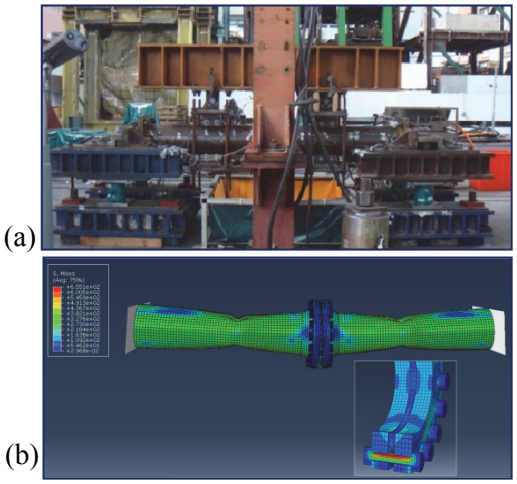


Fig. 2. (a) Pure bending test of the flange joint and (b) corresponding stress distribution in FEM analysis

International Communication of Research and Development of Earthquake Engineering between Taiwan and Haiti

Shiang-Jung Wang, Associate Researcher, NCREE

On January 12, 2010, a magnitude 7.0 earthquake occurred in Haiti. The epicenter was at a distance of 25 km southwest from Port-au-Prince, Haiti, and the focal depth was only about 13km. About one hundred thousand buildings collapsed, and most school and hospital buildings were destroyed. This earthquake caused around three hundred thousand casualties. Immediately, the Taiwan government and non-governmental organizations provided relief funds and goods together with assistance in rescue and medical treatment for the people of Haiti.

To provide more reliable seismic design codes and construction standards for building structures domestically, the Unit Housing and Public Buildings (UCLBP) was established directly under the Prime Ministry of Haiti. UCLBP officials attended the 2012 and 2013 IITP conferences held by NCREE, NARL in Taiwan. To review the performance of UCLBP, the First International Conference on Seismic Design of Structures (CICPS) was held in Port-au-Prince, Haiti, over January 10 and 11, 2014. Harry Adam, the executive director of UCLBP, invited a representative of NCREE to be a speaker at CICPS to share Taiwan's valuable experience in research and development of earthquake engineering. Dr. Wang, Shiang-Jung represented NCREE at CICPS and presented a talk entitled "Seismic Design for Structures with Isolation and Energy Dissipation Systems" (see Fig. 1). During CICPS, Dr. Wang also actively communicated with local officials, researchers and engineers. This participation in CICPS shows that Taiwan plays an important role in the research and development of earthquake engineering.

Great help was provided by the Taiwan Embassy in Haiti and was deeply appreciated. Dr. Wang made a courtesy call to Ambassador Lau and Premier Secretary Huang (see Fig. 2). Both sides concluded that a platform like CICPS is beneficial for Haiti's development and reconstruction and is worth encouraging in the future.



Fig. 1. Lecture and communication at CICPS



Fig. 2. Courtesy call to the Taiwan Embassy in Haiti: (left) with Ambassador Lau and (right) with Premier Secretary Huang

Introduction of Hydraulics Experiments for Pier Scouring

Meng-Huang Gu, Assistant Researcher, NCREE
Yung-Bin Lin, Research Fellow, NCREE

On January 15 and 17, 2014, hydraulics experiments were implemented in Xindian by the National Applied Research Laboratories (NARL). The aim of these hydraulics experiments is to test the integration of cross-field techniques for pier scouring issues. From a sensor node, the data stream was transmitted to the cloud server. After internal calculation by the server (Fig. 1), the related results were easily fed back to the platforms for display. From these procedures, it was verified that the integration of the cross-field technique is primarily a success.

The objective of the hydraulics experiments is to develop monitoring techniques for the issue of pier scouring. For this, the precipitation ensemble forecast techniques were applied to obtain rainfall data and to provide the boundary conditions for numerical simulation. The real-time forecast numerical model was developed to predict the water depth and discharge of a river. According to the above essential physical parameters, a bridge safety model was developed as a warning system. Furthermore, a large standard flume for assessing pier-scouring issues was also designed and built for testing the sensing system. Devices for wireless communication and data logging were constructed for remote control. Several sensing techniques were used to combine the sensor nodes for detecting real-time scouring depth. The navel pressure sensor was designed to study the forces on a pier under flooding. The related sensing data and forecasting results were integrated into the cloud server.

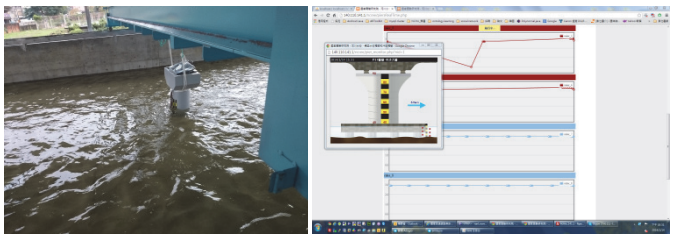


Fig. 1. The hydraulics experiment and results

Published by
National Center for Research on Earthquake Engineering
200, Sec. 3, XinHai Rd., Taipei 106, Taiwan, R.O.C.
Phone: 886-2-6630-0888
Fax: 886-2-6630-0858
Website: http://newsletter.ncree.org

The National Center for Research on Earthquake Engineering (NCREE) is a laboratory of National Applied Research Laboratories (NARL)
Website: http://www.narl.org.tw